

**TITLE:** Design of the Telescope Simulator imaging mirror

#### DISTRIBUTION

D Smith (RAL)  
B Swinyard (RAL)  
M Caldwell (RAL)  
P Gray (RAL)  
T Grundy (RAL)  
M Ferlet (RAL)

**CHANGE RECORD**

<b>ISSUE</b>	<b>SECTION</b>	<b>REASON FOR CHANGE</b>
1.0		

**CONTENTS**

1. Introduction.
2. Case of a mirror with biconic surface.
3. Case of a mirror with toroidal surface.
4. Alignment consideration
5. Mirror specification
  - 5.1. Mirror dimensions.
  - 5.2 Surface definition.

**APPLICABLE AND REFERENCE DOCUMENTS**

**RD1** Duncan et al., "Long wavelength (sub-mm) telescope simulator", Infrared Phys. 34-1 (1993)

**RD2** SPIRE-Technical Note: Telescope simulator optical design (to be issued as SPIRE-RAL-NOT 000 622, actually under ref. TOT\_S1V5\_b.doc)

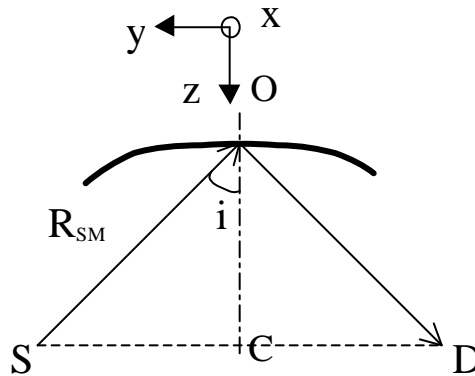
**RD3** SPIRE-Telescope simulator requirements specification.

### 1. Introduction

This note aims at presenting some practical solutions for the problem of 1:1 imaging between the source and the detector, giving recommendations for an adapted imaging mirror for the telescope simulator experiment, after taking into account the optical performances required as well as the manufacturing constraints.

### 2. Case of a mirror with biconic (ellipsoidal/spherical) surface

In the description of a previous telescope simulator in far-infrared range (R1), a spherical mirror was used off-axis. This leads to degradation of imaging performances as it introduces aberrations.



In order to have perfect imaging between the point source (S) and the detector (D), these points have to be located at the foci of an elliptically curved (in the plane yz) mirror. With an angle of incidence  $i$  for the incident beam at the mirror vertex O, the eccentricity  $e_y$  is given by  $e_y = \tan(i) = \sqrt{K_y}$  where  $K_y$  is the conic constant. In order to adapt the radius of curvature  $R_y$  to the wavefront radius of curvature given by the specified distance  $SO = R_{SM}$ , one needs to have  $R_y = R_{SM} * \sqrt{K_y + 1} = R_{SM} / \cos(i)$ . In the xz plane, the mirror can be just taken spherical ( $K_x = 0$ ) with its centre of curvature in C. Therefore the radius of curvature  $R_x$  is given by  $R_x = R_{SM} * \cos(i)$ . Applying these parameters at 45 deg of incidence, and with  $R_{SM} = 2100 \text{ mm}^1$ , we obtain  $K_x = 0$ ,  $K_y = 1$ ,  $R_x = 1484.92 \text{ mm}$ ,  $R_y = 2969.85 \text{ mm}$ .

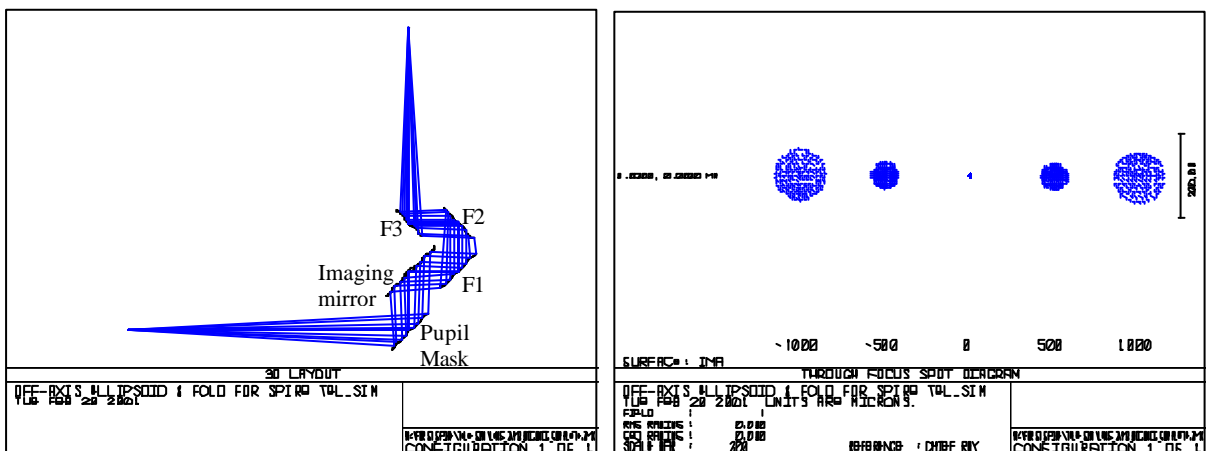


Figure 1: Zemax ray-tracing layout (yz plane) and spot diagrams around image surface for a test configuration

<sup>1</sup> This is an example value for  $R_{SM}$ . The definitive value has to be determined.

In Fig. 1, one can notice the quality of the image at the conjugate point of the point source. The displayed configuration uses the above values for the surface definition and  $R_{SM}$ . It also includes the mask (beam stop with an entrance pupil diameter set to  $\sim 199.5$  mm at 1729.5 mm from the source in order to simulate a system with  $F\# \sim 8.68$  as required), the imaging mirror under 45 deg of incidence, and a set of 3 fold mirrors (F1, F2 and F3). Longitudinal defocussing by  $\pm 1$  mm gives rise to a spot size no larger than  $100 \mu\text{m}$  (rms radius).

### 3. Case of a mirror with a toroidal surface

We consider now a surface having still 2 different radii of curvature  $R_x$  and  $R_y$  but spherical in both planes i.e. with  $K_x=K_y=0$ . The radii of curvature are still defined by the same definitions as above:  $R_x=R_{SM} \cdot \cos(i)$  and  $R_y=R_{SM}/\cos(i)$ . On-axis (normal incidence,  $i=0$ ), the surface becomes simply spherical with  $R_x=R_y=R_{SM}$  giving perfect imaging of the source. But practically, one has to use the mirror off-axis, introducing aberrations partially but not entirely attenuated by the toroidal surface shape. With  $i=20$  deg,  $R_x=1973.4$  mm and  $R_y=2234.8$  mm. Consequently, the beam size on the mirror is reduced (extension to  $\sim 300$  mm in diameter).

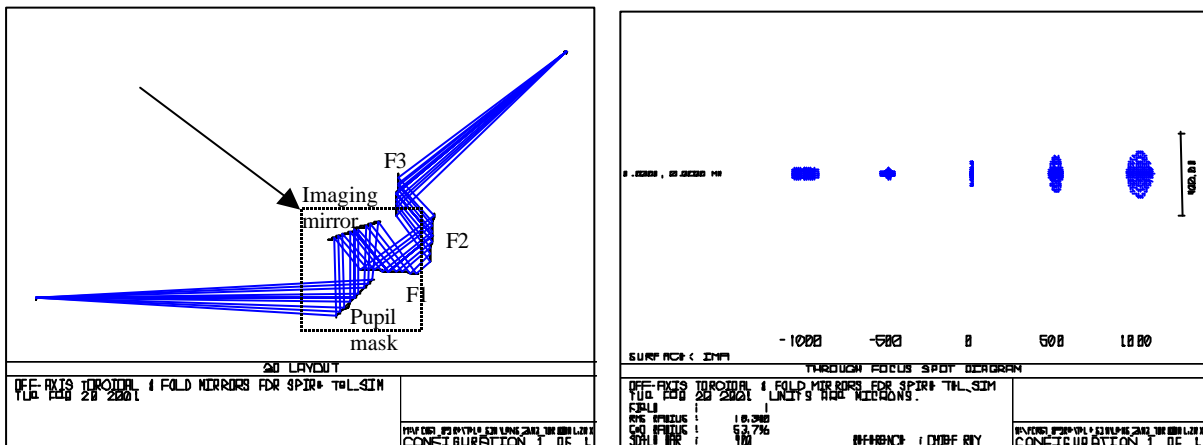


**Figure 2:** Zemax ray-tracing layout (yz plane) and spot diagrams for a second configuration ( $i=20$  deg)

In Figure 2, the effects of aberrations are seen on the spot diagrams. At the conjugate point, the beam has a linear extension and a better focus point can be chosen within  $\sim 0.5$  mm max before the conjugate point position. Although including some aberrations, the image of the point source remains smaller than  $100 \mu\text{m}$  in that configuration. But the large radial size of the beam and the constraints on the mask-mirror and mirror-first fold mirror distances can produce practical problems such as the incident beam impinging on the mirror may be partially diffracted by the first fold mirror edge (see dashed box in Fig 2, left). Even if the mask is used in transmission, there is necessity to increase either the mirror-F1 distance (set to 300 mm here) or the rotation angle (about x) for the imaging mirror so as to separate the incident and the reflected beam of the imaging mirror. As the distance between the mirrors can not be changed by much ( $\pm 50$  mm max for the beam control), the angle  $i$  should be increased and consequently the mirror size as well. In Figure 3, a configuration with  $i=35$  deg is displayed (mask used in transmission) where it can be seen that the incident beam on the imaging mirror will still be close to the edge of the first fold mirror F1. Therefore due to beam size and system geometry constraints,  $i$  needs to be larger than 35 deg (and smaller than 45 deg to keep the whole experimental set-up in a reasonable surface area). But spot pattern with the toroidal mirror degrades rapidly as  $i$  is increased. At

35 deg, the best focus would be mostly located  $\sim 2\pm 1$  mm away (longitudinally shifted) along the optical path and its rms size would already reach  $\sim 200$   $\mu\text{m}$  (getting even larger at  $i=45$  deg).

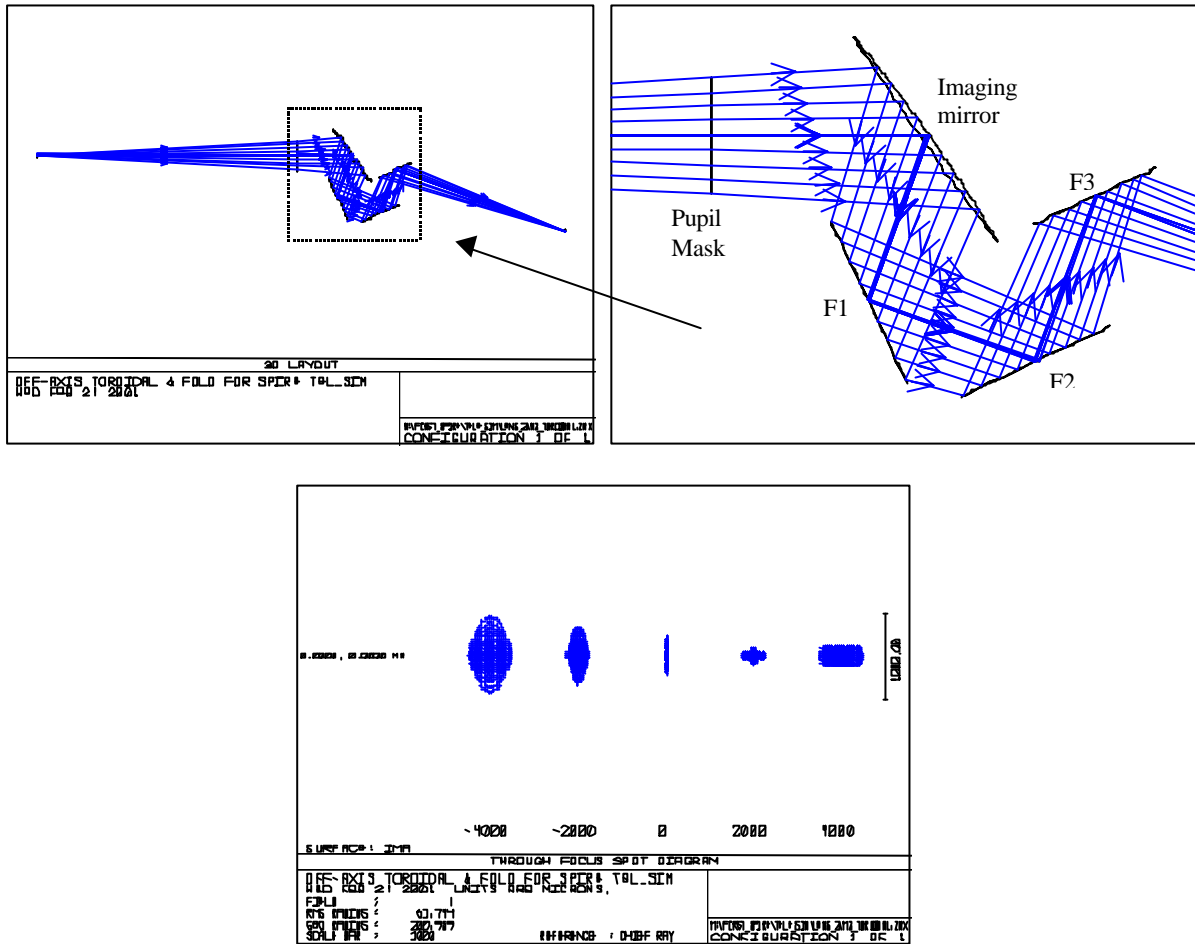
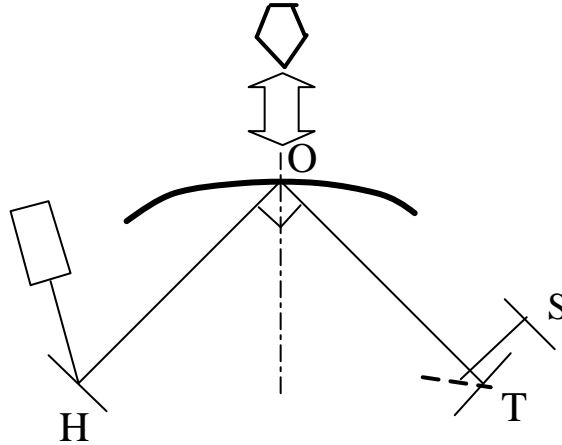


**Figure 3:** Zemax ray-tracing layout (yz plane) and spot diagrams for a configuration with  $i=35$  deg

#### 4. Alignment consideration

The previous discussion shows the necessity to work with an off-axis angle of at least 35 deg and no more than 45 deg. An angle of 45 deg seems to be better suited as it can be set with the use of a pentaprism. This will replace the first concept of locating foci of the mirror illuminating it on-axis then rotating it as the mirror (any of the 2 shape considered above) demonstrates poor optical imaging properties on-axis (too “slow” optics). A more detailed (step by step approach) alignment plan is under investigation and just a first possible draft concept is described below.



The visible laser + plate with hole (H) and the flat transfer mirror (T) can be set with reference to the optical bench (main level reference for the plane of propagation) with an autocollimator.

The pentaprism is used to set a 90 deg angle between the incident and reflected beam. Then the pentaprism is replaced by the mirror. Assuming existence of a mark locating the centre O of the mirror, the 3 points O, H and impact on T should be in the same plane. Verification could be made by use of a beam splitter + image surface to locate the second conjugate focus S (and tilt angle errors) after moving H along the path OH (measured distance; no need to it for OT) to the required  $R_{SM}$  (first focus point) distance (use of slide radius with expected accuracy smaller than 1mm). This required the visible laser signal to be strong enough (not too much scattered by mirror surface roughness and consequently there is a need for extra polishing around the centre of the mirror). Fine-tuning for the focus at detector plane could be made afterwards when inserting the 3 fold mirrors system that would allow final correction/adaptation of the second focus to detector. All this is actually placed under constrain of space made available (mainly determined by the chosen  $R_{SM}$  distance compared to the size of possible optical bench).

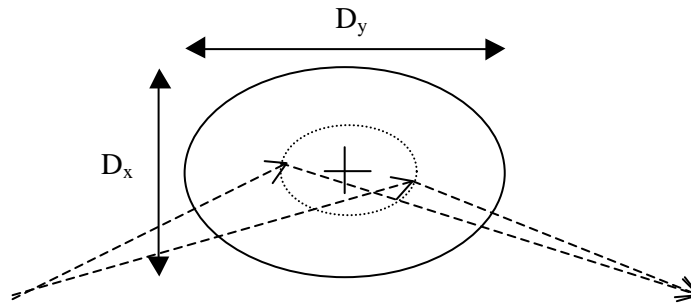
## 5. Specification of the mirror

From the considerations developed in the above paragraph, the case of an ellipsoidal mirror with a biconic surface seems to present to best optical properties with respect to the requirements and considering manufacturing difficulties which would be the same in both cases.

### 5.1. Mirror dimensions:

Mirror needs to be oversized with respect to the beam size on its surface to avoid loss by edge diffraction and spill-over. A factor 1.2 (20% oversized) is applied as a compromise between a too large size difficult and costly to manufacture and minimising the introduction of diffraction losses.

On-axis the beam impact on the mirror would be circular with a diameter  $\sim 242$  mm (also given by  $R_{SM}/F\#$ ). Therefore in the case presented in paragraph 1, we have  $D_x=300$  mm and  $D_y=425$  mm (the dimension is longer along y due to the angle of incidence  $i=45$  deg in yz plane).



High precision is not particularly requested on these dimensions but would be driven by the manufacturing constraints<sup>2</sup>. The mirror thickness should be at least 10 mm (due to the surface definition, see below, and dimensions) at the edge but 10% of the mirror size is commonly used which leads in this case to ~30 to ~40 mm of thickness at the mirror aperture edge.

In order to reduce the mirror dimensions without changing the system parameters ( $R_{SM}$ ,  $i$ ), a 10% oversize factor only could be applied instead of 20% because the propagation is relatively well “beamed”. A few percent loss may be expected through beam spreading due to diffraction over the free space optical path, which would affect mainly the longest working wavelength, as the diffraction coefficients varies with  $\lambda^{1/2}$ . This may need to be confirmed by further specific coherent beam pattern calculations. With this oversize smaller factor, the dimensions become  $D_x=275$  mm and  $D_y=390$  mm. These two sets of values would represent limits on the mirror dimensions for this value of  $R_{SM}$ . For lower values of  $R_{SM}$ , the mirror dimensions would decrease also as a good first-order estimation of the beam diameter of the mirror is given by  $R_{SM}/F\#$ .

### 5.2. Surface definition:

The sag  $z$  of the biconic surface is given the following equation:

$$z = \frac{c_x x^2 + c_y y^2}{1 + \sqrt{1 - (1 + K_x)c_x^2 x^2 - (1 + K_y)c_y^2 y^2}}$$

with  $c_x=1/R_x$  and  $c_y=1/R_y$  and  $K_x=0$ ,  $K_y=1$ ,  $R_x=1484.92$  mm and  $R_y=2969.85$  mm. Tolerancing with Zemax showed that  $R_x$  and  $R_y$  should be vary no more than a few mm from these nominal values in order to keep a rms spot size radius smaller than 0.1 mm at the image point (particularly  $R_y$ ). For the surface roughness, a max rms value taken as  $\lambda/20$  can be used. With the smallest working wavelength at ~200  $\mu\text{m}$ , that leads to ~10  $\mu\text{m}$  rms which is well achievable even over the entire large surface area. For alignment purposes, the central part of the mirror (disk of a few cm diameter around the middle) needs to be polished afterwards and should have a mark indicating the centre position. Cracks and surface defects may still remain after the polishing phase, and their sizes can cause some degradation (by surface scattering) of an alignment laser beam in the visible.

<sup>2</sup> The material is likely to be aluminium (lightweight, no corrosion) which leads to an approximate maximum weight of 7 kg for the large mirror. With this metallic material, a fractional power loss per reflection would be around 0.3% at  $\lambda \sim 300 \mu\text{m}$ .

Different manufacturers have been approached and among them, Thomas Keating Ltd would be able to machine such a large optical component with the above specification. An expected delivery time was estimated to 8 to 10 weeks and the price is under study.